

Energy state and micromechanical properties of PbO–ZnO–B₂O₃ glass-ceramic functional coatings on AISI420 stainless steel substrate

Z.Duriagina^{1,2}, T.Kovbasyuk¹, T.Bialopiotrowicz², S.Bespalov³

¹Lviv Polytechnic National University, 12 Bandrera St.,
79013, Lviv, Ukraine

²The John Paul II Catholic University of Lublin,
Al. Raclawickie 14, 20-950 Lublin, Poland

³Presidium of National Academy of Sciences of Ukraine,
55 Volodymyrska St., 03150 Kyiv, Ukraine

Received January 3, 2017

On AISI420 steel substrates with different roughness, PbO–ZnO–B₂O₃ glass crystalline functional coatings were synthesized by means of thick films method. The parameters of micro topography and values of free surface energy of the coatings and those of substrates surfaces have been investigated. The character of influence of substrates' micro topography and of free surface energy on the micromechanical properties of the synthesized coatings has been ascertained.

Keywords: thick films method, glass-crystalline functional coatings, PbO–ZnO–B₂O₃ glass-crystallin.

На підложках из стали AISI420 различной шероховатости методом толстых пленок синтезированы функциональные покрытия на основе стеклокристаллической системы PbO–ZnO–B₂O₃. Исследованы параметры микро топографии поверхности и рассчитано значение свободной поверхностной энергии получаемых покрытий и подложек. Установлен характер влияния микро топографии и поверхностной энергии подложек на микро механические свойства синтезированных покрытий.

Енергетичний стан та мікромеханічні властивості функціональних покриттів системи сталь AISI420 – склокераміка PbO-ZnO-B₂O₃. З.А. Дурягіна, Т.М. Ковбасюк, Т. Біалопіотрович, С.А. Бєспалов

На підкладках зі сталі AISI420 різної шорсткості методом товстих плівок синтезовано функціональні покриття на основі склокристалічної системи PbO–ZnO–B₂O₃. Досліджено параметри мікротопографії поверхні та розраховано значення вільної поверхневої енергії отриманих покриттів та підкладок. Встановлено характер впливу мікротопографії та поверхневої енергії підкладок на мікромеханічні властивості синтезованих покриттів.

1. Introduction

The most important properties which determine the quality of the coating are the high quality of micromechanical properties and its adhesion (adhesive strength) to a substrate [1]. There are many traditional methods for determining micro hardness,

Young's modulus, and other strength characteristics of coatings. However, these methods make it impossible to quantify the level of adhesive strength of coatings. For coatings synthesized by means of the method of thick films, determination of their adhesion strength concerning the substrate becomes still more difficult. In view of

this, to predict the adhesion strength of coatings, indirect methods of research can be used determining the surface free energy of substrates on which the coatings were synthesized [2]. Because it is known that the level of surface free energy determines the adhesive properties, this technique allows us to determine the levels of adhesion strength in the "coating-substrate" system, if provided the actual contact area between them is known.

In this work, functional coatings based on glass crystalline system $\text{PbO-ZnO-B}_2\text{O}_3$ on the AISI420 steel substrates with different parameters of surface roughness and micro topography were synthesized. Such coatings can be used as dielectric layer, which will be the basis for the application of the heating resistive coatings for flat heating elements (FHE) [3]. The 3D-topography and calculation of the of surface free energy values of the synthesized coatings and that of the substrates were obtained. The nature of an influence of the surface micro topography and parameters of free energy of substrates on the micromechanical properties of synthesized coatings were determined.

2. Experimental

2.1 Materials and experimental methods

For the synthesis of coatings, the AISI420 steel substrates with different values of roughness (S1 — automatic grinding ($R_z = 5.108 \mu\text{m}$); S2 — electrolytic etching ($R_z = 5.148 \mu\text{m}$); S3 — manual grinding ($R_z = 4.002 \mu\text{m}$)) were pretreated. AISI420 stainless steel was used as a substrate, because the values of the coefficients of thermal linear expansion of this steel and of the synthesized surface layers on the basis of sealants correlate with themselves properly [4].

The mixture of powders, whose contents are given in the Table 1, was used for coating. The obtained mixture was poured into alund crucible and melted at a temperature of 1180°C . After the time delay for 60 min at this temperature, the melt was quickly cooled in order to form amorphous structure and to avoid crystallization. The dried granulated substance was ground and sieved in order to obtain powder fraction with the particles size no greater than $56 \mu\text{m}$.

In order to produce a dielectric paste, 35...45 % of butyl acetate and 2...3 % of nitrocellulose varnish were added to the mixture of powders. The suspension was being mixed for 2...3 h in a ultrasonic mixer in order to form proper bonds among the particles. The obtained mixture was ap-

Table 1. Chemical composition of the initial powder

Oxide	Chemical content, mass% ($\pm 0.5 \%$)	
	SC 100-1	SC 90-1
PbO	75.5	75.3
ZnO	12	11.6
B_2O_3	8.4	8.5
SiO_2	2.1	2.1
Al_2O_3	2	0.8
BaO	—	1.7

plied to previously prepared surface of the substrate and dried at the temperature of 70°C . For the both coatings, the standard heat treatment with the two-stepped annealing at temperatures of 380 and 440°C and with holding at these temperatures for 45 min was performed. Heat treatment of coatings was conducted without protective atmosphere for activation of the oxides formation [3].

Our investigation of physical and mechanical properties was conducted by means of the method of continuous indentation with the use of a "Micron-gamma" device. The surface microtopography of the coatings and substrates was recorded by a "Micron-beta" interference profilometer over the surface area of 0.42 mm^2 [1]. Contact angles were measured using KSV Attension Theta (Biolin Scientific, Finland) optical tensiometer. The contact angle for at least 10 drops of every liquid.

2.2 Calculations of components and acid-base parameters of the surface free energy of the studied substrates

Van Oss et al. [5, 6] have considered the surface free energy of a solid and a liquid as the sum of the γ^{LW} component and of the γ^+ and γ^- parameters originated from the electron-acceptor (Lewis acid) and electron-donor (Lewis base), respectively. According this theory relationship between the contact angle and these components and parameters for a solid and a liquid is given by:

$$\gamma_L(\cos\theta + 1) = 2\sqrt{\gamma_S^{LW} \cdot \gamma_L^{LW}} + 2\sqrt{\gamma_S^+ \cdot \gamma_L^+} + 2\sqrt{\gamma_S^- \cdot \gamma_L^-} \quad (1)$$

A system of 3 equations like (1) for 3 liquids of known γ_L^{LW} , γ_L^+ and γ_L^- can be easily solved and the values of γ_S^{LW} , γ_S^+ and γ_S^- determined. From mathematical point of view, it is quite different situation

Table 2. The components and acid-base parameters of the surface free energy (mJ/m²) of used probe liquids

Liquid	Surface tension γ_L (mJ/m ²)	Lifshitz-van der Waals energy γ^{LW}		Energy of the acceptor's electron γ^+		Energy of the donor's electron γ^-	
		[11]	[12]	[11]	[12]	[11]	[12]
Water	72.8	21.8	21.8	65	25.5	10	25.5
Glycerol	64	34.4	33.6	16.9	12.21	12.9	18.06
Formamide	58	35.6	31.84	1.95	8.97	65.7	19.07
Ethylene glycol	48	31.4	29.76	1.58	2.76	42.5	30.13
Diiodomethane	50.8	50.8	50.8	0	0.72	0	0
1-Bromonaphtalene	44.4	44.4	44	0	0.39	0	0.48

if we have more than three liquids. In this case, we solve system of n ($n > 3$) equations in three unknowns. In this case, we have so called overdetermined system of linear equations, which is to be solved by the least square fitting. It was theoretically confirmed by Bialopirotowicz [7–10], that this method gives the lowest error in determination of the above-mentioned components and parameters.

For example, a system of equations for 6 liquids and 3 solids can be written as:

$$A_{6 \times 3} X_{3 \times 3} = B_{6 \times 3} \quad (2)$$

and corresponding matrices are as follows:

$$A = \begin{bmatrix} (\gamma_{L1}^{LW})^{1/2} & (\gamma_{L1}^-)^{1/2} & (\gamma_{L1}^+)^{1/2} \\ (\gamma_{L2}^{LW})^{1/2} & (\gamma_{L2}^-)^{1/2} & (\gamma_{L2}^+)^{1/2} \\ \dots\dots\dots \\ (\gamma_{L6}^{LW})^{1/2} & (\gamma_{L6}^-)^{1/2} & (\gamma_{L6}^+)^{1/2} \end{bmatrix}, \quad (3)$$

$$X = \begin{bmatrix} (\gamma_{S1}^{LW})^{1/2} & (\gamma_{S2}^{LW})^{1/2} & (\gamma_{S3}^{LW})^{1/2} \\ (\gamma_{S1}^+)^{1/2} & (\gamma_{S2}^+)^{1/2} & (\gamma_{S3}^+)^{1/2} \\ (\gamma_{S1}^-)^{1/2} & (\gamma_{S2}^-)^{1/2} & (\gamma_{S3}^-)^{1/2} \end{bmatrix}, \quad (4)$$

$$B = \frac{1}{2} \begin{bmatrix} \gamma_{L1}(1+\cos\theta_{L1}^{S1}) & \gamma_{L1}(1+\cos\theta_{L1}^{S2}) & \gamma_{L1}(1+\cos\theta_{L1}^{S3}) \\ \gamma_{L2}(1+\cos\theta_{L2}^{S1}) & \gamma_{L2}(1+\cos\theta_{L2}^{S2}) & \gamma_{L2}(1+\cos\theta_{L2}^{S3}) \\ \dots\dots\dots \\ \gamma_{L6}(1+\cos\theta_{L6}^{S1}) & \gamma_{L6}(1+\cos\theta_{L6}^{S2}) & \gamma_{L6}(1+\cos\theta_{L6}^{S3}) \end{bmatrix}. \quad (5)$$

Calculations of the γ^{LW} component and of the γ^+ and γ^- parameters for the studied solids were made using MATLAB version R2016b (MathWorks Inc., Natick, MA, USA), and presented above matrix equations were solved using the MATLAB function *pinv*, obtaining where *pinv*(*A*) is the Moore-Penrose pseudoinverse of the matrix *A*, *X* is the 3×3 matrix and *B* is 6×3 matrix of elements b_{ij}^0 (see Eqs. 3–5). All calculations were made using double precision:

$$X = \text{pinv}(A) \cdot B. \quad (6)$$

The contact angle values were measured for 6 probe liquids: water, glycerol, formamide, ethylene glycol, diiodomethane and 1-bromonaphtalene. Their surface tensions and γ^{LW} components and the γ^+ and γ^- parameters were listed in Table 2. Two sets of γ^{LW} components and the γ^+ and γ^- parameters for probe liquids were used. The first set was taken from Della Volpe and Siboni [11] paper. They claimed that this set better expresses acidic properties of water. The second set was taken from the Janczuk et al. paper [12]. Values of γ^{LW} components and the γ^+ and γ^- parameters for the studied solids calculated basing on the first set are named below as the method I and basing on the second set are named below as the method II.

3. Results and discussion

Investigation of surface topography of the generated coatings by the interference profilometer indicates similar nature of their structures (Fig. 1, a,b), regardless of microtopography of the substrates surfaces. SC 100-1 and SC 90-1 coatings have a homogeneous structure with great number of small cavities and needle formations 0.8...0.9 μm height. Surface roughness of SC 100-1 coating is of $Rz = 1.628 \mu\text{m}$, and for SC 90-1 of $Rz = 1.871 \mu\text{m}$. It should be noted that the thickness of the synthesized coatings varies in the range of 90...110 μm . Such a surface microtopography of dielectric coatings ensures high adhesive strength of the resistive layer which will applied to obtain FHE [3].

For predicting the adhesive strength of the dielectric coating to substrate, the surface topography and free surface energy of previously prepared substrates were studied

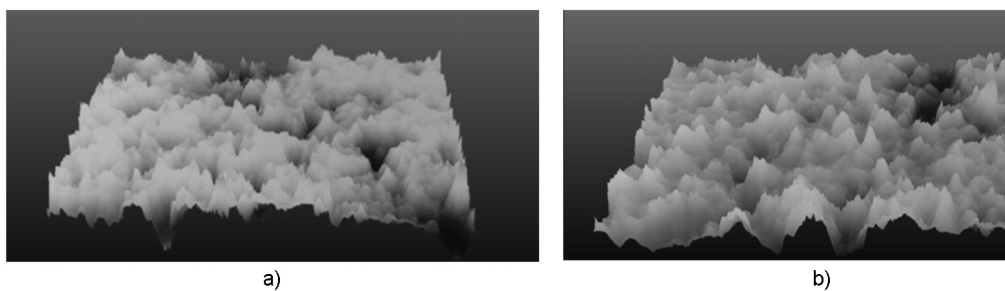


Fig. 1. Surface microtopography of functional coatings based on SC 100-1 (a) and SC 90-1 (b) powders on AISI420 steel substrates

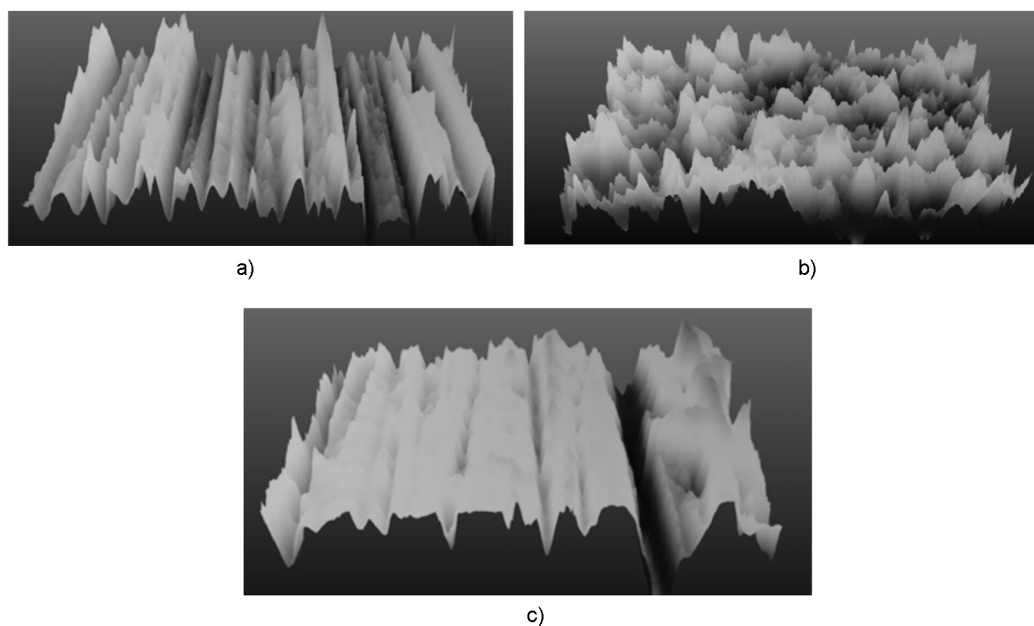


Fig. 2. Surface microtopography of AISI420 steel substrates after: a — automatic grinding (S1); b — electrolytic etching (S2); c — manual grinding (S3).

and calculated. The surfaces of the S1 and S3 substrates have a complicated irregular rectilinear microstructure with recesses and ridges 4.6...5.2 μm high (Fig. 2, a,c). The surface of the S2 substrate, obtained by electrolytic etching, has a homogeneous structure, and its topography (Fig. 2, b) is similar to the structure of the functional surfaces of SC 100-1 and SC 90-1 dielectric coatings. The height of the needle formations is uniformly and in average equals to 5.3 μm . Such a structure of substrate surfaces provides good adhesion for the synthesized dielectric layers. If the thickness of synthesized coatings is higher than 50...60 μm , the surface structure of the substrate does not affect their topography [3].

For calculation of surface free energy, we used the method of optical tensiometry with measurement of contact angles of drops of such probe liquids as: water, glyc-

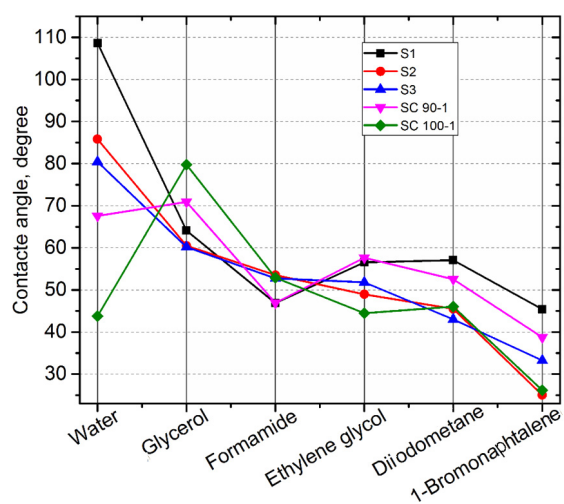


Fig. 3. Dependences of contact angles for the substrate S1, S2, S3 and coatings SC 90-1, SC 100-1 on the type of liquids.

Table 3. The components of surface free energy of S1, S2, S3 substrates and SC 90-1, SC 100-1 coatings

Substances and methods		Lifshitz-van der Waals energy γ^{LW} , (mJ/m ²)	Energy of the acceptor's electron γ^+ , (mJ/m ²)	Energy of the donor's electron γ^- , (mJ/m ²)	Total surface free energy γ^{tot} , (mJ/m ²)
SC 90-1	Method I	32.55	0.81	5.51	36.78
	Method II	27.94	0.03	21.59	29.55
SC 100-1	Method I	34.70	0.22	11.90	37.94
	Method II	27.57	0	36.22	27.57
S1	Method I	32,78	0.18	2.72	34.2
	Method II	34.77	1.38	4.84	39.9
S2	Method I	39.19	1.21	0.67	41.0
	Method II	36.92	2.46	1.11	40.2
S2	Method I	38.24	2.35	0.57	40.6
	Method II	34.90	7.42	0.37	38.2

erol, formamide, ethylene glycol, diiodomethane, 1-bromonaphthalene on the investigated surfaces. Figure 3 shows the changes of contact angles of the substrates S1, S2, S3 and of synthesized coatings depending on droplet fractions of liquid which were deposited onto the surfaces. The greatest average values of contact angles belong to S1 and S2 substrates. This indicates the dependence of the contact angle not only on the physical and chemical properties of the probe liquids, but also on the roughness and micro topography of the surface.

On the basis of the contact angle data, the surface free energies were calculated using of above-mentioned two methods. Table 3 shows calculated values of the components and acid-base parameters of surface free energy of S1, S2, S3 substrates and those of coatings which are based on PbO–ZnO–B₂O₃ glass crystalline system. The first method of calculation has given large scatter of the surface free energy data, by which it is difficult to predict the physical and mechanical properties of the investigated surfaces. According to the second method of calculation, the greatest values of the surface free energy belong to S1 and S2 substrates (Fig. 4). The surface free energy of SC 90-1 and SC 100-1 coatings, which were synthesized on those substrates, are low and amounted to 29.55 mJ/m² and 27.57 mJ/m², respectively. This confirms that the increase in a surface actual contact area occurs together with the increase of its roughness.

By means of microindentation technique, the Meyer's microhardness is determined, and the Young's modulus of SC 100-1 coat-

Table 4. The Meyer microhardness and Young's modulus of SC 100-1 coating depending on surface free energy of substrates

Surface free energy of substrates (mJ/m ²)	Meyer microhardness of SC 100-1 coating	Young's modulus of SC 100-1 coating (GPa)
38.2	5.62	71.6
39.9	5.361	73.96
40.2	4.98	64.85

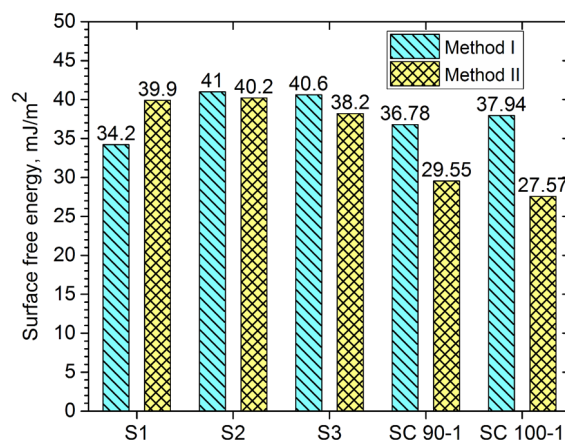


Fig. 4. Total surface free energy of S1, S2, S3 substrates and SC 90-1, SC 100-1 coatings.

ing depending on the surface free energy of previously prepared substrates is calculated. Microhardness of SC 100-1 coating varies in the range of 4.95–5.63 in a Meyer units scale. Moreover, the increase in free surface energy of substrates leads to the slight decrease in coatings' microhardness

(Table 4). Young's modulus values change in the range of 74.1...64.9 GPa. The fluctuations of the surface energy of substrates have not directly influenced on the change of Young's modulus, which depends mainly on the ratio of nano- and micro fragments of the formed coating structure. The coating which is applied onto S1 substrate has the highest Young's modulus value, because this substrate have most heterogeneous parameters of surface microtopography. This leads to the formation of a high number of crystallization centers during the synthesis process of functional coatings, and as consequence, to the formation of heterogeneous coatings microstructure with good strength properties [13, 14].

The present studies have shown that the micromechanical properties of functional coatings in the "AISI420 steel — PbO—ZnO—B₂O₃ system to a great extent depend on the microtopography and surface roughness of the substrate. The best adhesive strength and the highest value of Young's modulus of coatings are obtained when they are applied onto a substrate with the heterogeneous microstructure and roughness ($Rz = 5.108 \mu\text{m}$) of the surface obtained after mechanical grinding. The coatings obtained on the substrates after manual grinding ($Rz = 4.002 \mu\text{m}$) have the highest values of micro hardness with a simultaneous decrease in their values of Young's modulus. Synthesis of coatings on substrates which were prepared by electrolytic etching of surface ($Rz = 5.148 \mu\text{m}$) leads to the sharp decrease in microhardness and in values of the Young's modulus, as result of formation homogeneous microstructure of the surface layer [15, 16].

It is necessary to note that the method of thick films coating on substrates with roughness which exceeds $Rz = 10 \mu\text{m}$ leads to significant deterioration of the electro-insulating properties of coatings by significantly increasing the number of structural defects [17].

4. Conclusions

It is ascertained that the micromechanical properties of synthesized PbO—ZnO—

B₂O₃ coatings depend on the free surface energy, characteristic pattern of microtopography and on the surface roughness of the substrate. The increase in surface free energy of substrates provides high adhesion strength, similarly to the formation of a developed actual contact area between a coating and a substrate. Coatings which are synthesized on substrates with high heterogeneity of microtopography and the roughness Rz in the range of 4...5.5 μm have the highest values of microhardness and Young's modulus.

References

1. S.A.Firstov, S.R.Ignatovich, I.M.Zakiev, *Strength Mater.*, **41**, 147 (2009).
2. B.Janczuk, T.Bialopiotrowicz, E.Chibowski et al., *J. Mater. Sci.*, **25**, 1682 (1990).
3. Z.A.Duriagina, T.M.Kovbasyuk, S.A.Bespalov, *Usp. Fiz. Met.*, **17**, 29 (2016).
4. N.M.Pavlushkin, M.A.Kalmanovskaya, *Inorg. Mater.*, **12**, 2042 (1976).
5. C.J.vanOss, L.Ju, M.K.Chaudhury et al., *J. Colloid Interface Sci.*, **128**, 313 (1989).
6. C.J.vanOss, *Interfacial Forces in Aqueous Media*, Dekker, New York (1994).
7. T.Bialopiotrowicz, *J. Adhesion Sci. Technol.*, **21**, 1539 (2007).
8. T.Bialopiotrowicz, *J. Adhesion Sci. Technol.*, **21**, 1557 (2007).
9. T.Bialopiotrowicz, *J. Adhesion Sci. Technol.*, **23**, 799 (2009).
10. T.Bialopiotrowicz, *J. Adhesion Sci. Technol.*, **23**, 815 (2009).
11. C.Della Volpe, S.Siboni, *J. Colloid Interface Sci.*, **95**, 121 (1997).
12. B.Janczuk, T.Bialopiotrowicz, A.Zdziennicka, *J. Colloid Interface Sci.*, **211**, 96 (1999).
13. A.I.Ermolaeva, *Glass Phys. Chem.*, **27**, 306 (2001).
14. J.Honkamo, J.Hannu, H.Jantunen et al., *J. Electroceram.*, **18**, 175 (2007).
15. Z.A.Duriagina, T.M.Kovbasyuk, S.A.Bespalov et al., *Mater. Sci.*, **52**, 50 (2016).
16. Z.A.Duriagina, T.M.Kovbasyuk, M.Zagula-Yavorska et al., *Metallofiz. Noveishie Tekhnol.*, **38**, 1367 (2016).
17. Z.Duriagina, T.Kovbasyuk, M.Zagula-Yavorska et al., *Powder Metall. Met. C.*, **55**, 95 (2016).